

A State-Space Representation of Irradiance-Driven Dynamics in Two-Stage Photovoltaic Systems

Efstratios I. Batzelis , *Member, IEEE*, Georgios Anagnostou , *Member, IEEE*, and Bikash C. Pal , *Fellow, IEEE*

Abstract—In electric grids with large photovoltaic (PV) integration, the PV system dynamics triggered by irradiance variation is an important factor for the power system stability. Although there are models in the literature that describe these dynamics, they are usually formulated as block diagrams or flowcharts and employ implicit equations for the PV generator, thus requiring application-specific software and iterative solution algorithms. Alternatively, to provide a rigorous mathematical formulation, a state-space representation of the PV system dynamics driven by irradiance variation is presented in this paper. This is the first PV dynamic model in entirely state-space form that incorporates the maximum power point tracking function. To this end, the Lambert W function is used to express the PV generator's equations in an explicit form. Simulations are performed in MATLAB/Simulink to evaluate and compare the proposed dynamic model over the detailed switching modeling approach in terms of accuracy and computational performance.

Index Terms—Dynamic model, irradiance changes, Lambert W function, maximum power point tracking (MPPT), photovoltaic (PV) system, state-space model.

I. INTRODUCTION

CURRENTLY, power networks face difficulties from large-scale integration of renewables. Especially for photovoltaic (PV) systems, these challenges are associated with the dynamics driven by irradiance transients and grid disturbances [1]. For power system studies, there is a need for a robust and accurate model to describe the PV system response under these dynamic conditions [2].

There are several such dynamic models in the literature, greatly varying in the level of granularity they provide. In [3], the PV array is modeled without any power electronics taken into account. In [4] and [5], both the PV array and power converter are considered, but the maximum power point tracking

Manuscript received February 19, 2018; revised April 18, 2018 and May 15, 2018; accepted May 17, 2018. Date of publication June 14, 2018; date of current version June 19, 2018. The work of E. I. Batzelis was supported by the European Union's Horizon 2020 research and innovation programme under the Marie Skłodowska-Curie Grant 746638. The work of G. Anagnostou and B. C. Pal was conducted as part of the research project Joint UK India Clean Energy Centre, which is funded by the RCUK's Energy Programme (contract no.: EP/P003605/1). (Corresponding author: Efstratios I. Batzelis.)

The authors are with the Department of Electrical and Electronic Engineering, Imperial College London, London SW7 2AZ, U.K. (e-mail: e.batzelis@imperial.ac.uk; georgios.anagnostou1@imperial.ac.uk; b.pal@imperial.ac.uk).

This paper has supplementary downloadable material available at <http://ieeexplore.ieee.org>.

Color versions of one or more of the figures in this paper are available online at <http://ieeexplore.ieee.org>.

Digital Object Identifier 10.1109/JPHOTOV.2018.2839261

(MPPT) algorithm and other control modules are simplified or neglected; the entire power circuit and control scheme are taken into account in [1] and [6]–[9].

The latter approaches constitute the most accurate alternatives, since the MPPT dictates the dynamic response of the PV system under irradiance fluctuation and should not be ignored [1], [5]. However, although some differential equations are provided in [2], [4], [5], [9], and [10], all the above-mentioned models formulate some control functions through block diagrams or flowcharts; this is not a rigorous mathematical formulation and limits their applicability to specific software such as MATLAB/Simulink, DiGSILENT/PowerFactory, etc. Alternatively, a state-space representation is generally preferable, as it can be implemented into any software or platform and can be easily incorporated into a large power system study. However, to this day there is no state-space model in the literature that includes the MPPT function; they either neglect the MPPT or are not expressed entirely as a system of differential/difference and algebraic equations (DAEs).

Furthermore, the PV generator model adopted in the majority of these studies is simplified to facilitate calculations [1], [4], [6], [8]. The full single-diode model is considered only in [7], where the PV generator's equations are iteratively solved, which inevitably entails increased computational costs and numerical instabilities [7].

In this paper, a new model to represent the PV system dynamics triggered by irradiance variation is proposed, which is expressed in *entirely state-space* form. Although a state-space model, the *MPPT function is fully incorporated* by introducing a set of equivalent difference equations, while the Lambert W function is applied to achieve *explicit* formulation *without simplifying* the PV generator model. The initial state of the model is readily calculated through a simple straightforward procedure. Notably, this is the first PV dynamic model formulated as explicit state-space equations that do not neglect the MPPT or simplify the single-diode PV model. To evaluate the proposed model, simulations are performed in MATLAB/Simulink for two case studies using the detailed switching approach as a benchmark; the results show a significant gain in execution time and computational complexity at the same level of accuracy.

II. PROPOSED PV SYSTEM DYNAMIC MODEL

In two-stage PV systems (dc–dc converter and inverter), the response to irradiance variation is essentially determined by the PV generator and the dc–dc converter that actively participate

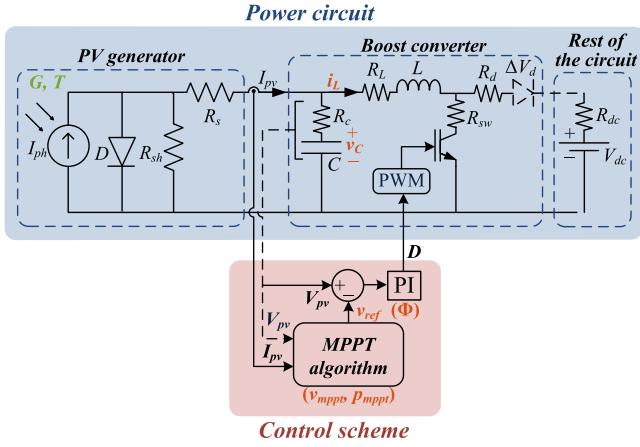


Fig. 1. Equivalent power circuit (blue background) and control scheme (red background) of a two-stage PV system.

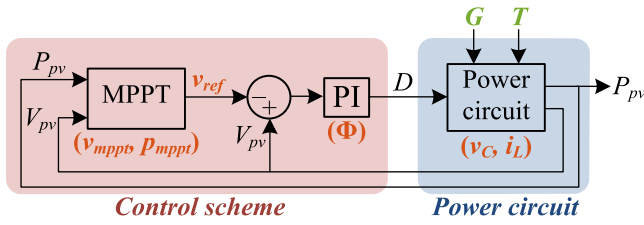


Fig. 2. Block diagram of the PV dynamic model. The model inputs are the irradiance G and temperature T , while the output is the extracted power P_{pv} .

in the energy extraction; the inverter does *not* contribute to the irradiance-driven dynamics. Therefore, the power circuit shown on blue background in Fig. 1 consists of the PV generator, modeled through the single-diode equivalent model, a boost converter, and an independent voltage source in place of the dc link and the rest of the ac circuit. A typical control scheme for these systems is considered, comprising a P&O MPPT algorithm and a voltage PI regulator (red background in Fig. 1).

The block diagram of the dynamic model proposed in this paper is depicted in Fig. 2. The entire *power circuit* is modeled as a single block (blue background) with three inputs (duty cycle D , irradiance G , and temperature T) and two outputs (PV power P_{pv} and voltage V_{pv}). The complete model of the PV system comprises the power circuit block (blue background) and the two control modules: MPPT and PI regulator (red background). The DAEs of these modules are described next.

A. PV Generator Model

The single-diode equivalent circuit of the PV generator is shown in a dashed-line frame in Fig. 1, characterized by the so-called *five parameters*: photocurrent I_{ph} , diode saturation current I_s , diode modified ideality factor a , series resistance R_s , and shunt resistance R_{sh} [11]. This describes any PV generator, from a cell to array, operating under uniform illumination. The conventional implicit current–voltage equation is given by

$$I_{pv} = I_{ph} - I_s \left(e^{\frac{V_{pv} + I_{pv} R_s}{a}} - 1 \right) - \frac{V_{pv} + I_{pv} R_s}{R_{sh}}. \quad (1)$$

This is an *algebraic equation*, since the PV generator dynamics are instantaneous [12]; yet, the nonlinear implicit form (V_{pv} and I_{pv} in both sides of the equation) necessitates numerical solution, which raises computational issues [7] and hinders incorporation into a state-space model. Recently, the Lambert W function $W\{x\}$ has been employed in static PV models to reformulate (1) and express I_{pv} as an explicit function of V_{pv} [11], [13]–[15]. However, for the state-space model of this paper, I_{pv} needs to be expressed as a function of the power circuit's state variables v_C and i_L , rather than V_{pv} :

$$I_{pv} = \frac{R_{sh} I_{ph} - v_C + R_c i_L}{R_s + R_c + R_{sh}} - \frac{a}{R_s + R_c} W \left\{ \frac{(R_s + R_c) R_{sh} I_s}{a(R_s + R_c + R_{sh})} e^{\frac{R_{sh} [(R_s + R_c) I_{ph} + v_C - R_c i_L]}{a(R_s + R_c + R_{sh})}} \right\} \quad (2)$$

$$V_{pv} = v_C - R_c (I_{pv} - i_L). \quad (3)$$

Note that (2) is similar to the one presented in [13] and [14], except for the use of R_c , v_C , and i_L in place of V_{pv} . Using (2) and (3), I_{pv} , V_{pv} , and thus $P_{pv} = V_{pv} I_{pv}$, can be directly calculated for given values of v_C and i_L , avoiding iterative numerical solution. The Lambert W function may be evaluated using the built-in MATLAB function *lambertw* or the series expansions proposed in [16]. To apply these equations, the five parameters need to be extracted at STC (1000 W/m²–25 °C) and translated to the actual irradiance G and temperature T . The details on these procedures are given in [11].

B. Average-Value Model of the Power Circuit

The *average-value model* of the power circuit in Fig. 1 is derived by averaging the voltage and current over a switching period [6], [7]. The well-known model for the boost converter includes two differential equations and two state variables: voltage of the input capacitor v_C and current of the inductor i_L :

$$\dot{v}_C = \frac{I_{pv} - i_L}{C} \quad (4)$$

$$\dot{i}_L = \frac{V_{pv} - (R_L + D R_{sw}) i_L - (1-D) [V_{dc} + \Delta V_d + (R_d + R_{dc}) i_L]}{L} \quad (5)$$

where C is the input capacitor's capacitance, L is the inductor's inductance, R_c , R_L , R_{sw} , R_d , and R_{dc} are the parasitic resistances of the circuit, V_{dc} is the constant dc-link voltage, and ΔV_d is the voltage drop on the diode, as shown in Fig. 1. The auxiliary variables V_{pv} and I_{pv} are calculated via the algebraic equations (2) and (3).

C. PI Controller Model

The state-space model of the PI controller is described by the following DAEs, involving one state variable Φ :

$$\dot{\Phi} = K_i (V_{pv} - v_{ref}) \quad (6)$$

$$D = \Phi + K_p (V_{pv} - v_{ref}) \quad (7)$$

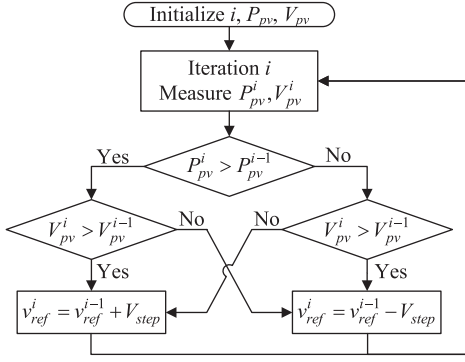


Fig. 3. Flowchart of a typical P&O MPPT algorithm.

where K_p and K_i are the proportional and integral gains of the regulator, and the term v_{ref} denotes the reference voltage determined by the MPPT control block (see Figs. 1 and 2).

D. P&O MPPT Model

The most commonly used MPPT algorithms in existing PV systems are still the P&O [9] and incremental conductance (INC) [6] methods. These are mostly modeled via flowcharts, rather than linear control blocks, due to their inherent algorithmic nature. The flowchart of a typical P&O algorithm is illustrated in Fig. 3: one iteration is performed every T_{mppt} seconds, adjusting the reference voltage v_{ref} by a constant value V_{step} . The sign of this adjustment is determined by whether the power was increased or decreased during the previous step.

In this form, the MPPT algorithm cannot be incorporated into a state-space model. To overcome this limitation, a state-space representation of the P&O method as discrete piecewise functions is proposed here (similar models can be derived for the INC and other MPPTs). Three state variables are introduced: the reference voltage v_{ref} , and the PV voltage v_{mppt} and power p_{mppt} recorded at the *previous* T_{mppt} period. The discrete equations, which describe the MPPT operation in Fig. 3, are

$$v_{ref}^k = \begin{cases} v_{ref}^{k-1} + \text{sign} \left(\frac{P_{pv}^{k-1} - P_{mppt}^{k-1}}{V_{pv}^{k-1} - v_{mppt}^{k-1}} \right) V_{step}, & \text{when } kT_s \bmod T_{mppt} = 0 \\ v_{ref}^{k-1}, & \text{otherwise} \end{cases} \quad (8)$$

$$v_{mppt}^k = \begin{cases} V_{pv}^{k-1}, & \text{when } kT_s \bmod T_{mppt} = 0 \\ v_{mppt}^{k-1}, & \text{otherwise} \end{cases} \quad (9)$$

$$p_{mppt}^k = \begin{cases} P_{pv}^{k-1}, & \text{when } kT_s \bmod T_{mppt} = 0 \\ p_{mppt}^{k-1}, & \text{otherwise} \end{cases} \quad (10)$$

where k is the discrete time instant, T_s is the discrete time step, *mod* denotes the modulo operation (remainder of Euclidean division), and the *sign* function returns $+1$ or -1 depending on the sign of the argument. The upper branch of the above-mentioned equations is evaluated only once per T_{mppt} period (when $kT_s \bmod T_{mppt} = 0$) to update the state variables according to the MPPT flowchart; the rest of the time, their values remain unchanged.

This way, the inherent discrete function of the MPPT is implemented. The variables v_{mppt} and p_{mppt} are only needed to keep track of the past operating point T_{mppt} seconds ago for (8).

E. Complete PV System Dynamic Model

The nonlinear time-invariant state-space model is formulated in discrete-time by a set of DAEs:

$$x^k = f(x^{k-1}, u^{k-1}) \quad (11)$$

$$y^k = h(x^k, u^k) \quad (12)$$

where x is the state vector, u is the input vector, and y is the output, in this case defined as

$$\begin{aligned} x &= [v_C \ i_L \ \Phi \ v_{ref} \ v_{mppt} \ p_{mppt}]^T \\ u &= [G \ T]^T \\ y &= P_{pv}. \end{aligned} \quad (13)$$

The state variables and inputs are indicated in red and green color, respectively, in Figs. 1 and 2. If the continuous times (4)–(6) are discretized and are combined with the discrete (8)–(10), a set of six difference equations are derived for (11):

$$v_C^k = v_C^{k-1} + \frac{I_{pv}^{k-1} - i_L^{k-1}}{C} T_s \quad (14)$$

$$\begin{aligned} i_L^k &= i_L^{k-1} + \frac{V_{pv}^{k-1} - (R_L + D^{k-1} R_{sw}) i_L^{k-1}}{L} T_s \\ &\quad - \frac{(1 - D^{k-1}) [V_{dc} + \Delta V_d + (R_d + R_{dc}) i_L^{k-1}]}{L} T_s \end{aligned} \quad (15)$$

$$\Phi^k = \Phi^{k-1} + K_i (V_{pv}^{k-1} - v_{ref}^{k-1}) T_s \quad (16)$$

$$v_{ref}^k = \begin{cases} v_{ref}^{k-1} + \text{sign} \left(\frac{P_{pv}^{k-1} - P_{mppt}^{k-1}}{V_{pv}^{k-1} - v_{mppt}^{k-1}} \right) V_{step}, & \text{when } kT_s \bmod T_{mppt} = 0 \\ v_{ref}^{k-1}, & \text{otherwise} \end{cases} \quad (17)$$

$$v_{mppt}^k = \begin{cases} V_{pv}^{k-1}, & \text{when } kT_s \bmod T_{mppt} = 0 \\ v_{mppt}^{k-1}, & \text{otherwise} \end{cases} \quad (18)$$

$$p_{mppt}^k = \begin{cases} P_{pv}^{k-1}, & \text{when } kT_s \bmod T_{mppt} = 0 \\ p_{mppt}^{k-1}, & \text{otherwise.} \end{cases} \quad (19)$$

The complete PV dynamic model consists of the *difference* equations (14)–(19) and the *algebraic* equations (2), (3), and (7) used for the auxiliary variables I_{pv}^{k-1} , V_{pv}^{k-1} , P_{pv}^{k-1} , and D^{k-1} . It is worth noting that, although explicit, this model is highly nonlinear and cannot be expressed in a matrix form.

F. Initialization of the Dynamic Model

In power system dynamics studies, the system is assumed to be on the steady state at the initial condition, meaning

TABLE I
PARAMETERS OF THE SIMULATED PV SYSTEM

Par.	Value	Par.	Value	Par.	Value	Par.	Value
P_{nom}	5 kW	V_{dc}	700 V	C	470 μ F	L	1.2 mH
R_L	0.01 Ω	R_C	0.3 Ω	R_{sw}	0.1 Ω	R_{dc}	0.0932 Ω
R_d	0.1 Ω	ΔV_d	0.1 V	I_{ph0}	15.88 A	I_{s0}	7.4e-10 A
a_0	18.34 V	R_{s0}	2.55 Ω	R_{sh0}	531.5 Ω	V_{step}	4.2 V
K_p	2.4e-5	K_i	0.12	F_c	20 kHz	F_{mppt}	10 Hz

that $\dot{x} = 0$ [17], [18]. Since in a discrete model $\dot{x} \approx (x^k - x^{k-1})/T_s$, the form of the difference equations (11) effectively becomes $x^0 = f(x^0, u^0)$ at the initial condition, where $x^0 = [v_C^0 i_L^0 \Phi^0 v_{ref}^0 v_{mppt}^0 p_{mppt}^0]^T$ is the initial state. This results in $i_L^0 = I_{pv}^0$ from (14), $v_C^0 = V_{pv}^0$ from (3), $\Phi^0 = D^0$ from (7), $v_{ref}^0 = V_{pv}^0$ from (16), $v_{mppt}^0 = V_{pv}^0$ from (18), and $p_{mppt}^0 = P_{pv}^0$ from (19), where the initial duty cycle D^0 is found from (15):

$$D^0 = \frac{V_{dc} + \Delta V_d + (R_d + R_{dc} + R_L) I_{pv}^0 - V_{pv}^0}{V_{dc} + \Delta V_d + (R_d + R_{dc} - R_{sw}) I_{pv}^0}. \quad (20)$$

Furthermore, in the steady state the PV generator operates at the maximum power point (MPP). Therefore, I_{pv}^0 and V_{pv}^0 are essentially the MPP current I_{mp} and voltage V_{mp} , respectively, found in an explicit way by [11]

$$V_{pv}^0 = V_{mp} = (1 + R_s/R_{sh}) a (w - 1) - R_s I_{ph} (1 - 1/w) \quad (21)$$

$$I_{pv}^0 = I_{mp} = I_{ph} (1 - 1/w) - a (w - 1) / R_{sh} \quad (22)$$

where w is a coefficient calculated via the parameters I_{ph} and I_s using the Euler's number e and the Lambert W function $W\{x\}$

$$w = W\{I_{ph} e / I_s\}. \quad (23)$$

Therefore, the initial state is given by

$$x^0 = [V_{mp} \ I_{mp} \ D^0 \ V_{mp} \ V_{mp} \ P_{mp}]^T \quad (24)$$

which is readily calculated through the explicit (20)–(23). This is a straightforward procedure that does not require any iterative or numerical solution.

III. CASE STUDIES AND SIMULATION RESULTS

To validate the proposed dynamic model, simulations are performed in MATLAB/Simulink for a 5 kW PV system corresponding to the circuit in Fig. 1. The system parameters are given in Table I. In the following, the dynamic response of the system is simulated for two case studies of fast irradiance variation using both the proposed state-space (SS) model and the detailed switching (SW) alternative (see also Supplementary videos). For the former, the equations in Section II are applied with a time step of 100 μ s, while for the latter, the circuit in Fig. 1 is simulated at two different time steps: 10 and 100 ns.

A. Sudden Increase in Irradiance

In the first case study, the PV system experiences a sudden increase in irradiance from 600 to 1000 W/m^2 within 1.2 s,

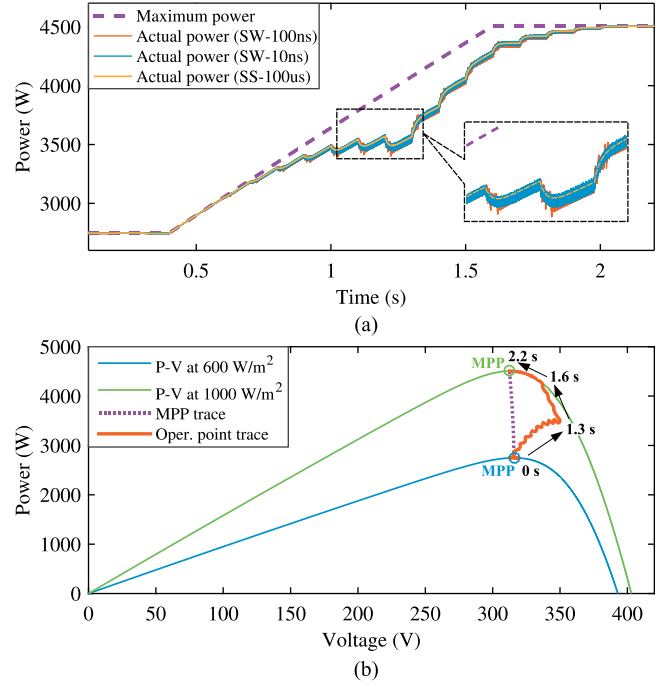


Fig. 4. Case study A: Sudden increase in irradiance. (a) Maximum and actual output power. (b) P - V curve and trace of the operating point.

which corresponds to a day with frequent changes in cloud cover [19]. This irradiance fluctuation is reflected to the maximum available power shown in purple dashed line in Fig. 4(a). The actual output power resulting from the two runs of the SW model (10/100 ns—blue/red lines) is essentially the same, except for limited fluctuation during MPPT steps in the second case; the results are very similar to the SS model (yellow line), the latter providing accurately the system dynamic response apart from the switching ripple. The deviation between the maximum and actual output power is noteworthy, especially at 0.9–1.8 s; this is due to the erroneous operation of the P&O algorithm, which fails in tracking the MPP during abrupt irradiance changes.

To further investigate this phenomenon, the trace of the operating point on the time-varying P - V curve is illustrated with red color in Fig. 4(b). Initially, the operating point oscillates around the MPP of the blue-colored curve (600 W/m^2). As the irradiance increases up to 1000 W/m^2 , the P - V characteristic is gradually modified providing more power, effectively becoming the green-colored curve. The MPP trace during this transient is indicated by the purple dotted line. However, the MPPT regulates the operating point toward the wrong direction until 1.3 s (red line), when the direction is corrected and slowly converges to the new MPP. This is a well-known malfunction of conventional MPPTs [5], [7] that considerably affects the dynamic response of the system [see Fig. 4(a)]. Yet, several relevant models in the literature neglect the MPPT function and assume that the operating point lies on the MPP trajectory (ideal MPPT) [1]–[4], [10], resulting in inaccurate modeling of the dynamic response. This highlights the need to properly include the MPPT in PV dynamic modeling studies.

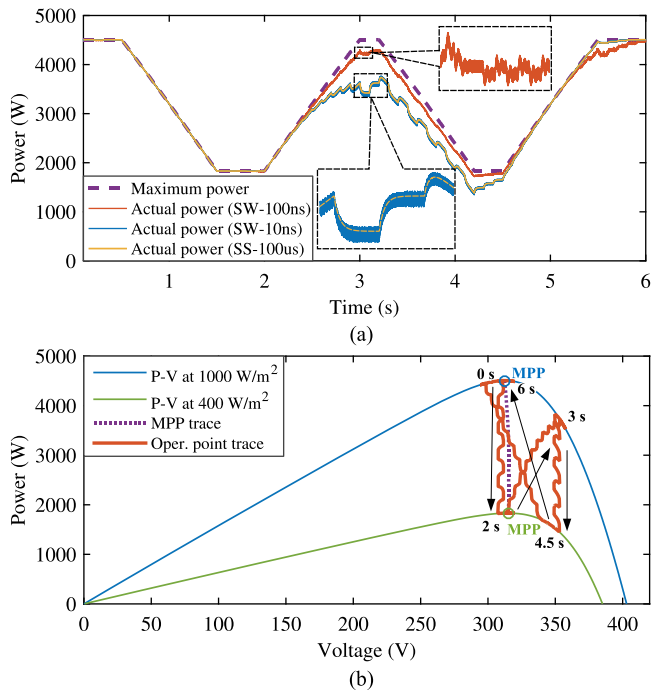


Fig. 5. Case study B: *Repeated irradiance variation*. (a) Maximum and actual output power. (b) P - V curve and trace of the operating point.

TABLE II
COMPARISON OF THE SWITCHING AND STATE-SPACE MODELS

Execution time	Time step	Case study A	Case study B
Switching (SW) model	10 ns	~45 m (2,715 s)	~2 h (7,207 s)
Switching (SW) model	100 ns	~6 m (340 s)	~14 m (846 s)
State-space (SS) model	100 μ s	1.5 s	2.5 s

B. Repeated Irradiance Variation Caused by Passing Clouds

The second study-case scenario considers a more intense irradiance fluctuation between 1000 and 400 W/m² caused by passing clouds. The maximum and actual output power are depicted in Fig. 5(a): the SS model results (yellow line) almost coincide with the SW-10 ns model (blue line), both deviating from the red dashed line for some time. It is worth noting that in this case, the outcomes of the two runs of the SW model do not coincide, with the larger time step (red line) resulting in inaccurate modeling of the dynamic response under very fast irradiance variation; this is indicative of the challenges related to the selection of the time step in a switching model.

The P - V curves and the trace of the operating point are displayed in Fig. 5(b). Even though the MPP is shifted almost vertically while the irradiance changes (purple dotted line), the operating point takes a zigzag-like path (red line) as the black arrows indicate. This once more stresses the need to include the MPPT in a PV dynamic model.

IV. COMPUTATIONAL PERFORMANCE

To evaluate and compare the calculation cost of the two models, the execution time of the two study-case scenarios is recorded and presented in Table II. Both mod-

els are built and simulated in MATLAB/Simulink R2016a (SimPowerSystems toolbox, accelerator simulation mode), in a PC with a 3.5-GHz CPU and 64-GB RAM. The SW model is simulated at two necessarily very small steps: 10 and 100 ns to produce high-resolution pulsewidth modulation pulses (20 kHz switching frequency—see Table I). On the contrary, a much larger simulation step of 100 μ s is allowed for the SS model, just slightly less than the time constants of the differential equations involved.

Table II shows that the proposed SS model is executed approximately 2000–3000 times faster than the SW-10 ns, and 200–300 times faster than the SW-100 ns. The larger the time step of the SW model, the less the computational effort, albeit at the cost of reduced accuracy, as discussed in Section III. By adopting the SS model instead, the time step selection is no longer limited by the switching frequency, exhibiting high accuracy at a very low simulation time.

V. CONCLUSION

In this paper, a new dynamic model to describe the PV system response to irradiance changes is proposed. The model is described entirely in the SS form, including the MPPT function, and consists of explicit equations that employ the Lambert W function. Simulations in MATLAB/Simulink reveal highly accurate results and show considerable gain in computational efficiency and complexity over the detailed SW modeling approach. This investigation verifies that the MPPT function is a crucial factor for the irradiance-driven dynamics of a PV system and needs to be included in PV dynamic modeling studies. The mathematically rigorous formulation of the proposed dynamic model permits implementation to any computational platform and facilitates incorporation into large power system studies.

REFERENCES

- [1] R. Shah, N. Mithulananthan, R. C. Bansal, and V. K. Ramachandaramurthy, "A review of key power system stability challenges for large-scale PV integration," *Renew. Sustain. Energy Rev.*, vol. 41, pp. 1423–1436, Jan. 2015.
- [2] D. Remon Rodriguez, A. M. Cantarellas, and P. Rodriguez, "Equivalent model of large-scale synchronous photovoltaic power plants," *IEEE Trans. Ind. Appl.*, vol. 52, no. 6, pp. 5029–5040, Nov. 2016.
- [3] S. Koohi-Kamali, N. A. Rahim, H. Mokhlis, and V. V. Tyagi, "Photovoltaic electricity generator dynamic modeling methods for smart grid applications: A review," *Renew. Sustain. Energy Rev.*, vol. 57, pp. 131–172, May 2016.
- [4] S. Mishra and D. Ramasubramanian, "Improving the small signal stability of a PV-DE-dynamic load-based microgrid using an auxiliary signal in the PV control loop," *IEEE Trans. Power Syst.*, vol. 30, no. 1, pp. 166–176, Jan. 2015.
- [5] V. N. Lal and S. N. Singh, "Control and performance analysis of a single-stage utility-scale grid-connected PV system," *IEEE Syst. J.*, vol. 11, no. 3, pp. 1601–1611, Sep. 2017.
- [6] X. Mao and R. Ayyanar, "Average and phasor models of single phase PV generators for analysis and simulation of large power distribution systems," in *Proc. 24th Annu. IEEE Appl. Power Electron. Conf. Expo.*, Washington, DC, USA, Feb. 2009, pp. 1964–1970.
- [7] A. Yazdani *et al.*, "Modeling guidelines and a benchmark for power system simulation studies of three-phase single-stage photovoltaic systems," *IEEE Trans. Power Del.*, vol. 26, no. 2, pp. 1247–1264, Apr. 2011.
- [8] P. P. Dash and M. Kazerani, "Dynamic modeling and performance analysis of a grid-connected current-source inverter-based photovoltaic system," *IEEE Trans. Sustain. Energy*, vol. 2, no. 4, pp. 443–450, Oct. 2011.

- [9] N. Hamrouni, M. Jraidi, A. Dhouib, and A. Cherif, "Design of a command scheme for grid connected PV systems using classical controllers," *Electr. Power Syst. Res.*, vol. 143, pp. 503–512, Feb. 2017.
- [10] M. J. E. Alam, K. M. Muttaqi, and D. Sutanto, "A multi-mode control strategy for VAR support by solar PV inverters in distribution networks," *IEEE Trans. Power Syst.*, vol. 30, no. 3, pp. 1316–1326, May 2015.
- [11] E. I. Batzelis, "Simple PV performance equations theoretically well-founded on the single-diode model," *IEEE J. Photovolt.*, vol. 7, no. 5, pp. 1400–1409, Sep. 2017.
- [12] P. G. Bueno, J. C. Hernández, and F. J. Ruiz-Rodríguez, "Stability assessment for transmission systems with large utility-scale photovoltaic units," *IET Renew. Power Gener.*, vol. 10, no. 5, pp. 584–597, May 2016.
- [13] G. Petrone, G. Spagnuolo, and M. Vitelli, "Analytical model of mismatched photovoltaic fields by means of Lambert W-function," *Sol. Energy Mater. Sol. Cells*, vol. 91, no. 18, pp. 1652–1657, Nov. 2007.
- [14] M. L. Orozco-Gutierrez, J. M. Ramirez-Scarpetta, G. Spagnuolo, and C. A. Ramos-Paja, "A technique for mismatched PV array simulation," *Renew. Energy*, vol. 55, pp. 417–427, Jul. 2013.
- [15] Y. Mahmoud and E. F. El-Saadany, "Fast power-peaks estimator for partially shaded PV systems," *IEEE Trans. Energy Convers.*, vol. 31, no. 1, pp. 206–217, Mar. 2016.
- [16] E. I. Batzelis, I. A. Routsolias, and S. A. Papathanassiou, "An explicit PV string model based on the Lambert W function and simplified MPP expressions for operation under partial shading," *IEEE Trans. Sustain. Energy*, vol. 5, no. 1, pp. 301–312, Jan. 2014.
- [17] G. Anagnostou and B. C. Pal, "Derivative-free Kalman filtering based approaches to dynamic state estimation for power systems with unknown inputs," *IEEE Trans. Power Syst.*, vol. 33, no. 1, pp. 116–130, Jan. 2018.
- [18] K. R. Padiyar, *Power System Dynamics*. Hyderabad, India: BS Publications, 2008.
- [19] K. Gibson, I. R. Cole, B. Goss, T. R. Betts, and R. Gottschalg, "Compensation of temporal averaging bias in solar irradiance data," *IET Renew. Power Gener.*, vol. 11, no. 10, pp. 1288–1294, Aug. 2017.



Georgios Anagnostou (M'17) was born in Athens, Greece. He received the Diploma in electrical and computer engineering from the National Technical University of Athens, Athens, Greece, the M.Sc. degree in sustainable energy futures and the Ph.D. degree in electrical engineering from Imperial College London, London, U.K., in 2011, 2012, and 2016, respectively.

His current research interests include power system dynamics and control, dynamic security assessment, dynamic state estimation, and renewable energy based generation.

Dr. Anagnostou is a member of the Technical Chamber of Greece.



Bikash C. Pal (M'00–SM'02–F'13) received the B.E.E. (with honors) degree from Jadavpur University, Calcutta, India, the M.E. degree from the Indian Institute of Science, Bangalore, India, and Ph.D. degree from Imperial College London, London, U.K., in 1990, 1992, and 1999, respectively, all in electrical engineering.

He is currently a Professor with the Department of Electrical and Electronic Engineering, Imperial College London. His current research interests include renewable energy modeling and control, state estimation, and power system dynamics.

Dr. Pal was the Editor-in-Chief of the IEEE TRANSACTIONS ON SUSTAINABLE ENERGY (2012–2017) and Editor-in-Chief of IET Generation, Transmission and Distribution (2005–2012). He is a Fellow of the IEEE for his contribution to power system stability and control.



Efstratios I. Batzelis (S'14–M'17) received the M.Eng. degree from the Technical University of Crete (TUC), Crete, Greece, and the M.Sc. and Ph.D. degrees from the National Technical University of Athens (NTUA), Athens, Greece, in 2009, 2012, and 2016, respectively, all in electrical engineering.

During 2016–2017, he was a Postdoctoral Researcher with NTUA and then with Imperial College London (ICL), U.K. He is currently a Marie Curie Research Fellow with ICL, working on his project "PVCi – Photovoltaic control and integration." His

current research interests include renewable energy technologies and distributed generation, especially photovoltaics, inverter and power system control.